J. Fluid Mech. (2005), *vol.* 544, *pp.* 173–200. © 2005 Cambridge University Press
doi:10.1017/S0022112005006609 Printed in the United Kingdom

On the flow-induced Marangoni instability due to the presence of surfactant

By HSIEN-HUNG WEI

Department of Chemical Engineering, National Cheng Kung University, Tainan 701, Taiwan

(Received 28 February 2005 and in revised form 14 June 2005)

The flow-induced Marangoni instability due to the presence of surfactant is examined for long-wavelength perturbations. A unified view of the underlying mechanisms is provided through revisiting both falling film and two-fluid Couette flow systems. The analysis is performed by inspecting the corresponding coupled set of evolution equations for the interface and surfactant concentration perturbations. While both systems appear to have very similar sets of equations consisting of base flows and Marangoni effects, the origins of stability/instability are identified and illustrated from a viewpoint of vorticity. The base flow rearranges the surfactant distribution and the induced Marangoni flow tends to stimulate the interface's growth. But this destabilizing effect is reduced by effects combining the interface travelling motions and the Marangoni recoil. The competition between these opposing effects determines the system stability, and is elucidated using equations in concert with observations from initial value problems. Moreover, a criterion for the onset of instability can be established in line with the same rationale. The present work not only furnishes a lucid way to clarify the instability mechanisms, but also complements previous studies. Extension to the weakly nonlinear regime is also discussed.

1. Introduction

The stability of interfacial flow is a subject of longstanding fundamental interest in fluid dynamics and engineering applications. Since most interfacial flow systems contain surface-active agents or surfactants, their roles in affecting the system stability are often critical to processes. This article is devoted to understanding and clarifying the stability mechanisms of surfactant-laden interfacial flow.

It is believed that the dominant effect of surfactant on the stability is due to Marangoni forces that drive the fluid from low-surface-tension to high-surface-tension regions. For stationary planar systems, surfactant effects are damping (Berg & Acrivos 1965) in analogy to thermocapillary stabilization (Pearson 1958). In the presence of a base flow, Whitaker & Jones (1966, hereafter referred to as WJ) first examined the effect of surfactant on the long-wave instability of a falling film flow. They showed that surfactant could have a stabilizing effect such that the critical Reynolds number, beyond which the system is stable, increased with surfactant elasticity. Pozrikidis (2003) extended the analysis to arbitrary-wavelength disturbances and found that for zero Reynolds numbers surfactant could make the system less stable compared to the surfactant-free case. For two-fluid systems, Frenkel & Halpern (2002, hereafter referred to as FH) studied the effect of surfactant on the long-wave instability of a two-layer Couette flow in the limit of Stokes flow. They found that surfactant can induce destabilization to a system that is inherently stable without surfactant. Extension to

the case with arbitrary wavenumbers was made in their subsequent analysis (Halpern & Frenkel 2003). In related work, Blyth & Pozrikidis (2004, hereafter referred to as BP) developed a lubrication-flow model to examine both linear and nonlinear stabilities for long-wavelength perturbations. In addition to verifying the features of linear instability found by FH, they showed that the Marangoni instability could be arrested by nonlinear effects under certain conditions. Wei (2005*a*) recently extended the analysis of WJ by applying an additional shear stress on the interface. He found that a stable clean-interface system could be destabilized by surfactant, depending on the direction and strength of an applied surface shear.

All these early studies suggest that surfactant can influence the system stability due to its interaction with base flows. The role of base flows in affecting the stability of surfactant-laden systems lies in the interfacial tangential stress condition and the surfactant transport equation. The first gives rise to a jump in the base shear stress across the interface, providing a perturbation shear stress that can induce a flow. The second is primarily due to surface convection that can rearrange the surfactant distribution along the interface. The surface convection has two parts: one comes from perturbations to the basic interfacial velocity, and the other is simply attributed to the surface flow created by Marangoni forces. For falling film flow as in WJ, the surface velocity is induced by the first mechanism and then re-distributes surfactant through the second. The resulting Marangoni effect is stabilizing to the system. On the other hand, for a two-fluid system as in FH, there is no contribution from the first mechanism; most of the surfactant is rearranged by the perturbation of the basic interfacial velocity. In contrast to a single-fluid falling flow, Marangoni effects could cause destabilization in a two-fluid system.

As pointed out by FH, the main cause of a Marangoni destabilization is the interfacial shear of a base flow. However, for a falling film flow although its basic interfacial shear is zero, a perturbation to it can have similar advective effects on the surfactant rearrangement. But this does not lead the system to be unstable. The instability mechanism given by FH only reflects a part of the story. As we shall demonstrate, both falling film and two-fluid Couette flow systems produce very similar sets of evolution equations governing the long-wave stability. Two-fluid systems involve further complication due to viscosity stratification. Technically speaking, in all the equations the surface velocities contain terms that are proportional to the deflection of the interface. Since such a term can cause a stabilizing effect in one case but the opposite in another, similar physical effects can lead to different outcomes. This requires clarification, which is the main theme of this article.

In this work, we aim to offer a unified view to explain the situation above. To do this, we revisit the long-wavelength stabilities of both vertically falling film flow and two-fluid Couette flow systems in the presence of surfactants (see figure 1). Although similar systems have been analysed previously by WJ, FH and BP, the formulations of these studies were less tractable so that the interpretations had to rely on either special-case illustrations (FH) or numerical observations (BP), and were thus less obvious. The present ansatz will utilize the lubrication-flow formulation to derive a set of linear evolution equations relevant for each case. As we shall show, the derived sets of evolution equations appear to be in rather simple forms in comparison with these previous studies. This enables us to more easily identify the underlying physics and to expedite the interpretations based on the equations. The paper is organized as follows. We first examine a single-layer falling film with surfactant in § 2. A two-fluid Couette flow with surfactant is examined in § 3. In § 4 we briefly discuss the extension to the weakly nonlinear regime. Concluding remarks are made in § 5.

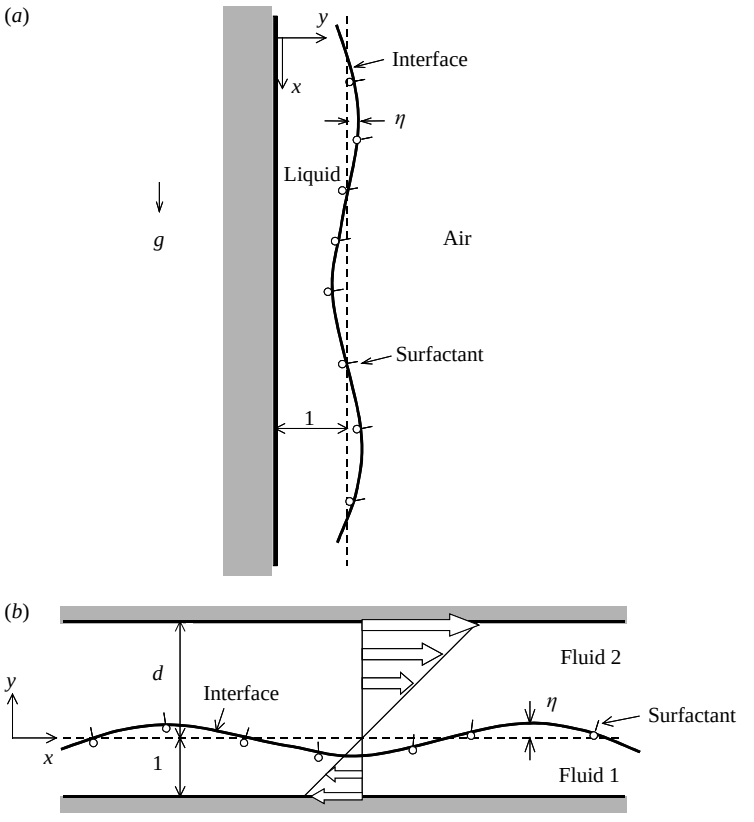

FIGURE 1. Surfactant-laden flow systems. (*a*) One-fluid vertically falling film flow. (*b*) Two-fluid Couette flow.

2. Vertically falling film flow with surfactant

2.1. *Problem formulation*

The purpose of this study is to identify the origin of the flow-induced instability due solely to the presence of surfactant. To isolate Marangoni effects, henceforth we consider a liquid layer flowing down a vertical plane, see figure 1(*a*). This allows us to eliminate stabilizing effects due to hydrostatic pressures. We also restrict our attention to a flow system with negligible inertia so that destabilizing effects due to inertia are excluded in the problem. The liquid of density ρ^* and viscosity μ^* is covered by a monolayer of insoluble surfactant. To non-dimensionalize the system, the unperturbed depth of the liquid layer h^* and the unperturbed interfacial velocity $U_0^* = \rho^* g^* h^*/(2\mu^*)$ (with g^* being the gravitational acceleration) are chosen as the characteristic length and velocity scales, respectively. The pressure is scaled by $\mu^* U_0^*/h^*$. Time has a scale of h^*/U_0^*. The flow system is defined in Cartesian coordinates aligned with the plane: x points down the slope, and y is the outward direction normal to the wall defined at $y = 0$. Let u and v be the velocity components in the x- and y-directions, respectively, and p be the pressure. The base flow is given by $U = 2y - y^2$. For perturbations with a small wavenumber k ($\ll 1$), the governing equations are

$$u_x + v_y = 0, \tag{1}$$

$$0 = -p_x + u_{yy}. \tag{2}$$

Here the perturbation pressure p is a function only of x as a consequence of $p_y = 0$ in the leading-order y-momentum equation. Let η and Γ denote the perturbations to the interface and the uniform surfactant concentration, respectively. The latter is scaled by the surfactant concentration Γ_0^* in the base state, and σ_0^* is the corresponding surface tension. For the normal stress balance condition at the interface, p arising from surface tension forces is $\eta_{xx}Ca^{-1} \sim k^2Ca^{-1}$ where $Ca = \mu^* U_0^*/\sigma_0^*$ is the capillary number. If $Ca \geqslant O(1)$, $p_x \sim k^3/Ca$ in (2) is at most $O(k^3)$; thus the surface-tension-driven flow can be negligible. This enables us to examine the effects arising only from interactions between surfactant and the base flow. The tangential stress balance at the interface gives

$$u_y(y=1) = -U_{yy}|_{y=1}\eta - M\Gamma_x, \tag{3}$$

where $M = -\Gamma_0^*/\sigma_0^*(\partial\sigma^*/\partial\Gamma^*)_{\Gamma_0^*}/Ca$ is the Marangoni number. Equation (3) suggests that a Marangoni force can drive u at $O(k)$. According to (2), p_x is $O(k^3)$, hence so is the corresponding u. We therefore can neglect p_x in (2) for assessing only the Marangoni-driven instability. As a result, applying $u(y=0) = 0$ at the wall and (3) yields the perturbation flow field:

$$u = (2\eta - M\Gamma_x)y,\ v = \left(-\eta_x + \tfrac{1}{2}M\Gamma_{xx}\right)y^2. \tag{4}$$

This flow field is then substituted into the kinematic condition $v(y=1) = \eta_t + U(y=1)\eta_x$ and the surfactant transport equation $\Gamma_t + U(y=1)\Gamma_x + U_y|_{y=1}\eta_x + (u(y=1))_x = 0$ at the unperturbed interface. The latter equation is applied for insoluble surfactant with negligible surface diffusion. Also note that $U_y|_{y=1} = 0$. In a reference frame moving with the basic interfacial velocity, i.e. $x \to x - U(y=1)t$, we arrive at the following set of evolution equations that govern the long-wave stability of the system:

$$\eta_t + \eta_x - \tfrac{1}{2}M\Gamma_{xx} = 0, \tag{5}$$

$$\Gamma_t + 2\eta_x - M\Gamma_{xx} = 0. \tag{6}$$

The effects of the base flow are reflected by the terms η_x and $2\eta_x$ in (5) and (6), respectively. These terms are derived from the perturbation to the basic shear stress $U_{yy}|_{y=1}\eta$ due to the interface deflection as indicated by (3). Applying normal modes $(\eta, \Gamma) = (\hat{\eta}, \hat{\Gamma})\exp(\mathrm{i}kx + st)$ to the above set of equations yields two linear growth rates $s = 0$ and $s = -(\mathrm{i})k + Mk^2)$. The first mode has a zero growth rate, suggesting that surfactant could make the system less stable. This mode seems to have been overlooked previously until the recent study by Pozrikidis (2003). The second mode corresponds to the result of WJ which is the correction to Yih's clean-interface study (Yih 1963).

2.2. *Vorticity interpretation of instability mechanism*

The mechanism of instability can be generally interpreted using eigenfunctions. In contrast to the previous studies (FH, BP), a more appropriate interpretation based on eigenfunctions would be given from the viewpoint of vorticity. This concept was first proposed by Hinch (1984) to explain the shear-induced instability of two immiscible fluids, and later applied to surfactant-free, falling film systems (Huang & Khomami 2001; Kelly *et al.* 1989). Charru & Hinch (2000) extended the idea and provided a unified view for the instability of two-layer Couette flows. How vorticity determines instability depends on its phase difference relative to the interface. Since this concept appears to be quite general, it is worthwhile explaining how it works in more detail.

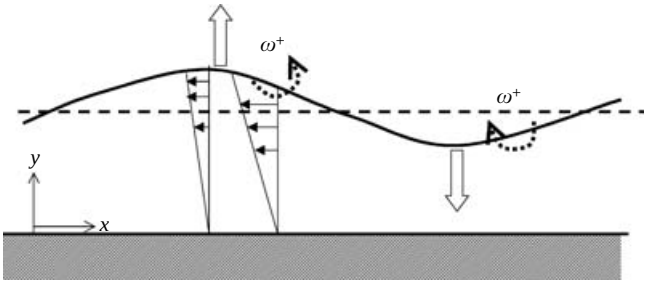

FIGURE 2. Explanation of stability mechanism from the viewpoint of the vorticity–interface phase difference. The leading-order vorticity is given by $\omega = -u_y$. ω^+ and ω^- denote the maximum and the minimum vorticities, respectively. Consider the case when vorticity is ahead of the interface deflection. For a control volume between a peak and the ω^+ end of the interface the flow induced at the peak is weaker than that at the ω^+ end, giving rise to upward motions of the peak. Similar reasoning leads the trough move downwards. As a result, the interface deflection amplifies, leading to an unstable system.

We take a falling film flow as an example. Using (4), the leading-order perturbation vorticity ω is given by

$$\omega = -u_y = -2\eta + M\Gamma_x. \tag{7}$$

Thus ω remains uniform across the film. Stability/instability can be identified by whether perturbation vorticity leads or lags behind the interface deflection. The mechanism is illustrated by figure 2. Let θ denote the phase difference of perturbation vorticity relative to the interface deflection. For $\theta > 0$, the extremes of positive (negative) vorticity are located at the surface points somewhat ahead of the interface peaks (troughs). Now consider a control volume enclosing a peak and its adjacent maximum-vorticity location. In this enclosed region, because the perturbation vorticity is counterclockwise, it induces backward fluid motions. Since the vorticity at the peak is weaker, the flow entering across the maximum-vorticity end is greater than that leaving the peak end. The resulting net flow is thus positive, amplifying the interface deflection at the peak. Similar reasoning also holds at the interface trough. Therefore, $\theta > 0\,(<0)$ leads the system to be unstable (stable). Alternatively, how vorticity induces fluid motions that affect the interface dynamics can be seen directly from the kinematic condition $\eta_t = v(y = 1) = \frac{1}{2}\omega_x$ in connection with vorticity using (4) and (7). That is, vorticity causes fluid motions normal to the unperturbed interface. In the normal-mode form, we have

$$\hat{\omega} = 2k^{-1}(s_i - \mathrm{i}s_r)\,\hat{\eta}, \tag{8}$$

where s_r and s_i denote the real and imaginary parts of the growth rate s, respectively. Hence the vorticity–interface phase difference θ is given by

$$\theta = \mathrm{sign}(s_i)\mathrm{Arg}(s_i - \mathrm{i}s_r), \quad -\pi \leqslant \theta \leqslant \pi. \tag{9}$$

To identify whether vorticity leads ($\theta > 0$) or lags behind ($\theta < 0$), the interface should be frame viewed in a reference of the propagating direction (via $\mathrm{sign}(s_i)$) of the interface. For a forward-propagating interface, $s_i < 0$, it follows that $\theta > 0\,(<0)$ requires $s_r > 0\,(<0)$ for instability (stability) as illustrated earlier. If the interface travels backwards, i.e. $s_i > 0$, then instability (stability) occurs when $\theta < 0\,(>0)$.

In the absence of surfactant ($M = 0$), although Kelly *et al.* (1989) have explained this case, we will provide an alternative explanation, not only for completeness but also for the later comparison with the surfactant case. ω is generated by the perturbation

shear stress $U_{yy}|_{y=1}\eta$ due to the base flow. Positive (counterclockwise) vorticity arises for $\eta < 0$ with its maximum at the interface troughs whereas negative (clockwise) vorticity prevails for $\eta > 0$ with its extreme at the interface peaks. That is, ω is out of phase with η. Since vorticity has no variation at the peaks or troughs, its induced fluid motions do not produce any net flows across these points; the interface deflection neither grows nor shrinks. The system therefore remains neutral.

When surfactant is present, since the Marangoni stress drives the fluid to move backwards (forwards) for $\Gamma_x > 0\,(<0)$, it modifies vorticity in a counterclockwise (clockwise) sense as indicated by (7). For the growth rate $s = 0$, the corresponding eigenfunction yields $\hat{\Gamma} = -2\mathrm{i}\hat{\eta}/Mk$, suggesting that Γ leads η by $\pi/2$. As revealed by (7), the vorticity created by the Marangoni effect lags behind Γ by $\pi/2$; this vorticity is thus in phase with η, offsetting the out-of-phase vorticity created by the basic shear stress. Because both in-phase and out-of-phase vorticities cancel out exactly, ω is zero. Since a zero vorticity does not induce any fluid motions, the system simply remains neutral. For the growth rate $s = -(\mathrm{i}k + Mk^2)$, we find $\hat{\Gamma} = 2\hat{\eta}$. The normal-mode vorticity $\hat{\omega} = 2\hat{\eta}(-1 + Mik)$ suggests that vorticity lags behind the interface, hence giving rise to a stabilizing effect.

FH and BP proposed mechanisms based on Marangoni forces to explain instability in two-fluid systems, but applying a similar mechanism as theirs to falling film flow would be less clear. For example, the $s = 0$ eigenfunction suggests that the Marangoni effect draws the fluid toward or away from the interface mid-points, tending to an unstable interface growth. However, as we shall demonstrate later, how this destabilizing action can make the system unstable depends on its competition with instability reducing effects. Accounting only for this destabilizing effect without including attenuating mechanisms as these studies did could lead to an inconsistent interpretation.

While vorticity appears useful to explain stability/instability, the eigenfunctions are determined *a posteriori* from the derived equations. Their features already reflect interplay among a variety of factors involved; the origin of the eigenfunctions still needs an explanation. In the next subsection we shall provide an alternative view to the problem. The interpretation will be based on the evolution equation with the aid of observations using the initial value problem approach. This furnishes a more direct way to envisage how a base flow interacts with surfactant so as to determine the system stability.

2.3. *Initial value problem*

The system is initially subjected to a sinusoidal perturbation of the interface. The initial surfactant concentration remains uniform. To solve (5) and (6) numerically, assuming $\eta = A(t)\cos(kx) + B(t)\sin(kx)$ and $\Gamma = C(t)\cos(kx) + D(t)\sin(kx)$, we can reduce them to a set of ordinary differential equations with appropriate initial conditions for unknown time-dependent coefficients A, B, C, and D. This set of equations is then solved numerically using the Gear method.

Figure 3 shows the developments of both the interface and surfactant concentration. According to (4), the perturbation to the interface yields a perturbed surface velocity that is proportional to the deflection of the interface. This surface velocity (via $2\eta_x$ of (6)) rearranges the surfactant distribution; it increases (decreases) the surfactant concentration on the interface portions where $\eta_x < 0\,(>0)$. The resulting surfactant concentration has maxima or minima at the interface mid-points, but no variation at the interface crests or troughs. That is, the surfactant distribution has a phase of $\pi/2$ ahead of the interface. This is also equivalent to the $s = 0$ eigenfunction $\hat{\Gamma} = -2\mathrm{i}\hat{\eta}/Mk$.

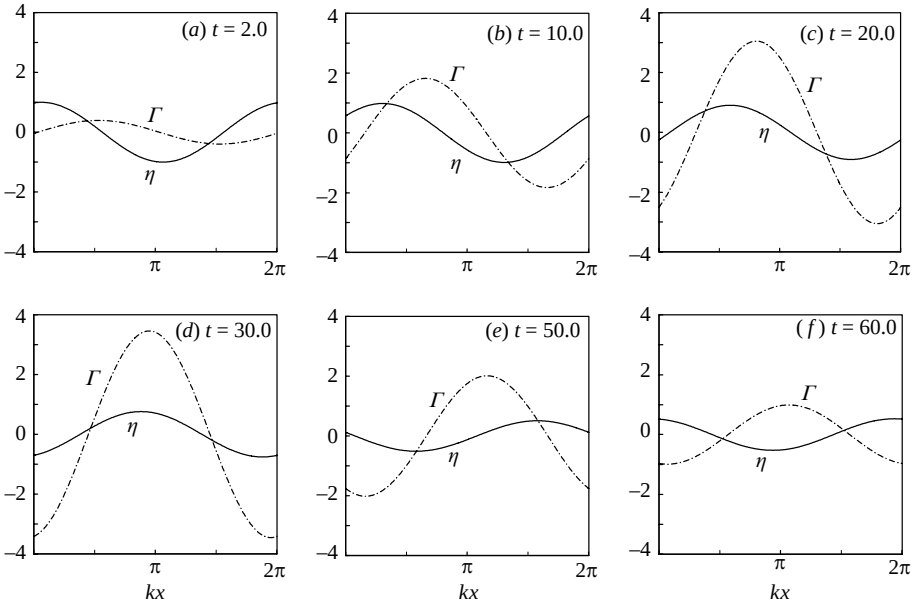

FIGURE 3. The spatio-temporal evolution of η and Γ for a falling film flow. $M = 1$, $k = 0.1$.

Such a configuration lasts for short time (figure 3*a*). When the induced Marangoni forces dominate the travelling term η_x in (5), they tend to increase (decrease) η on the portions where $\eta_x > 0\,(<0)$. So the induced interface growth takes the form of a backward-travelling wave. It is shown in figure 3(*b*) that η lags behind Γ slightly. However, the base flow effect, via η_x of (5), causes the interface to travel forwards. This forward-travelling wave can offset the above growth tendency due to the Marangoni effects (figure 3*c*) because $-\eta_x$ and Γ_{xx} are out of phase. In addition, the developing Marangoni flow also tends to reduce the surfactant concentration gradient in view of the diffusion nature of (6), opposing the concentration steepening due to η_x in (5). When these reducing effects are stronger than the Marangoni-induced growth, the interface deflection gradually fades away, as does the surfactant concentration perturbation (figure 3*d–f*).

The above observations also can be interpreted in conjunction with figure 4 for the temporal behaviours of the amplitudes of η, Γ and ω. Let δ be the amplitude of the initial perturbation to the interface. At the very early stages of the evolution during which the amplitude of Γ is not large, (5) suggests $\eta_t + \eta_x = O(k^2)$; that is, the interface travels slowly without a change in its amplitude during the time scale $t \sim O(k^{-1})$. Meanwhile, since $\Gamma_t + 2\eta_x = O(k^2)$ from (6), such a slowly changing interface leads the surfactant concentration to grow like $\Gamma \sim \eta_x(t=0)t \sim k\delta t$ and the corresponding Marangoni effect to $M\Gamma_{xx} \sim k^3 M\delta t$ within the time scale of $O(k^{-1})$ (i.e. $kt \lesssim \pi$ in figure 4). When time is about to reach a scale of $O(k^{-2}M^{-1})$ (about $kt \sim 2\pi$ in figure 4), the amplitude of Γ becomes sufficiently large and is of $O(k^{-1}M^{-1}\delta)$. This order is also consistent with the $s = 0$ eigenfunction $\hat{\Gamma} = -2\mathrm{i}\hat{\eta}/Mk$. At this stage, the Marangoni influences start to be comparable to the effects due to the η_x terms.

At the later stages when $t \geqslant O(k^{-2}M^{-1})$, the gradient of Γ is reduced by strong Marangoni diffusion ($M\Gamma_{xx}$ of (6)), so the Γ amplitude decreases. The resulting Marangoni flow becomes weaker, as does its tendency to stimulate the interface

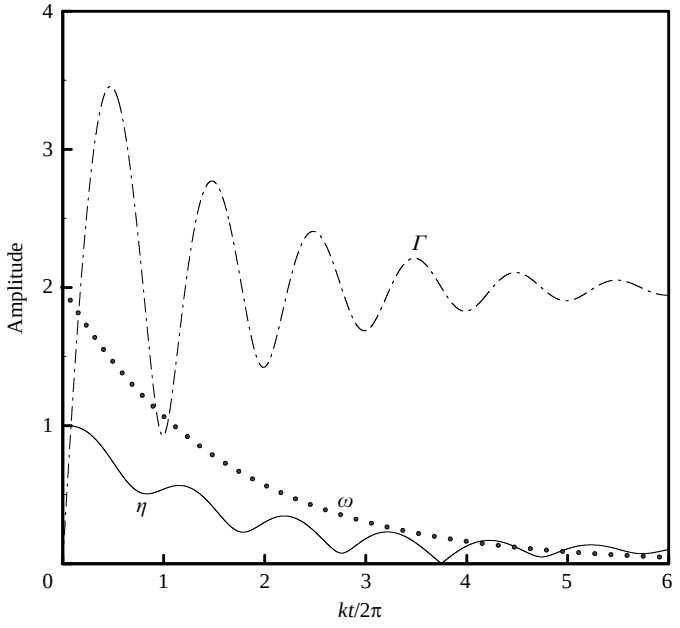

FIGURE 4. The temporal evolution of the amplitudes of η, Γ and ω corresponding to figure 3.

growth (through $M\Gamma_{xx}/2$ of (5)). Since this growth is not strong enough to compete with the travelling-wave depletion to furnish the subsequent interfacial growth, the interface amplitude decreases (or increases slightly for a short period of time). This further weakens the subsequent Marangoni forces, reducing the tendency of interface growth. Repeating the above process thus gradually damps the interface perturbations in successive cycles. Damping is even more evident when observing the temporal evolution of vorticity; the vorticity decays exponentially with time. This, via (7), indicates that the vorticity created by the interface deflection is offset by that of the Marangoni stress. Figure 5 shows the evolution of both $\Gamma-\eta$ and $\omega-\eta$ phase differences. These results are plotted in the range between $-\pi$ and 2π to track their changes with time in a continuous manner. Note that when the phase θ is larger than π, it should be read as a phase lag of $(2\pi-\theta)$. The long-time $\Gamma-\eta$ phase difference approaches $\pi/2$, which is consistent with the $s=0$ eigenfunction $\hat{\Gamma}=-2\mathrm{i}\hat{\eta}/Mk$. The corresponding $\omega-\eta$ phase difference changes rapidly between 0 and 2π, indicating that the vorticity has no preference regarding leading nor lagging behind the interface, hence the system remains neutral.

Note that the above transitory growth prior to long-term decay has not been addressed previously for falling film system. Since a similar dynamic transition was also found by BP for two-fluid systems, we believe that similar competing mechanisms should also appear in two-fluid systems as we shall demonstrate later.

2.4. *Instability mechanisms*

As demonstrated above, the key to stability is two competing mechanisms: (i) the flow-induced steepening of the surfactant concentration and the Marangoni interface growth, and (ii) the interface-travelling-wave depletion and the Marangoni relaxation effect on the surfactant concentration. As such, the reason why the system (5) and (6) is neutrally stable can be briefly explained as follows. An interface growth due to the base-flow-induced Marangoni effect is offset by a travelling interface wave.

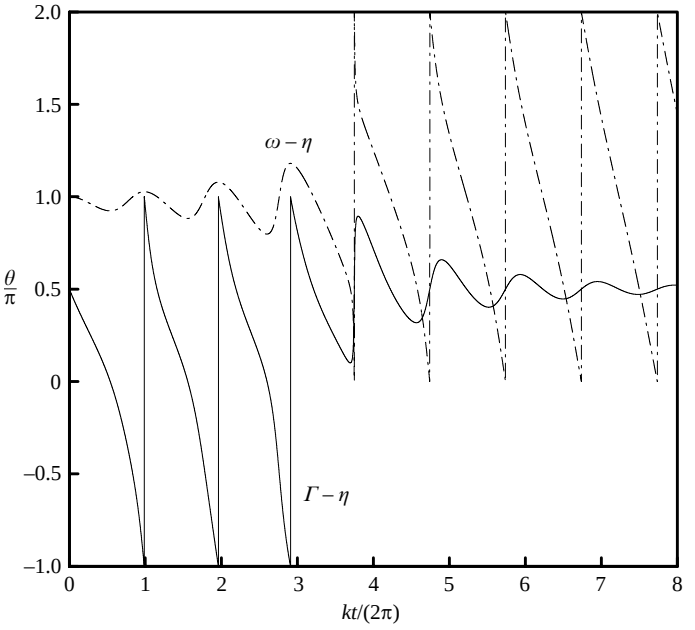

FIGURE 5. The temporal evolution of the phase differences $\Gamma - \eta$ and $\omega - \eta$ corresponding to figure 3. The phase θ is plotted in the range $-\pi < \theta < 2\pi$ to track its change with time in a continuous manner. Note that θ larger than π should be read as a phase lag of $(2\pi - \theta)$.

The resulting interface becomes almost stationary and tends to steepen the surfactant concentration. But this concentration steepening is again completely balanced by the Marangoni diffusion.

In comparison with the evolution-equation-based argument above, the use of eigenfunctions cannot describe the interaction during the growth–decay transition period at the early stages of the evolution. We have demonstrated that to understanding this transition is important because it shows how competing effects determine the fate of the system. In this regard, it is more appealing to use the evolution-equation-based interpretation in concert with initial value problems for elucidating the underlying physics.

A neutrally stable falling film with surfactant is a consequence of exactly balancing actions between destabilizing effects and those that reduce them; an imbalance could lead to an instability. To illustrate this, we first consider (5) with the following artificial change of the travelling-wave term:

$$\eta_t + \lambda\eta_x - \frac{M}{2}\Gamma_{xx} = 0, \tag{10}$$

where λ is a measure of the wave speed. Inspecting the real part of the normal-mode growth rate, we find that the system is unstable for $\lambda < 1$. Since the Marangoni-induced growth is accompanied by a backward-travelling interfacial motion, a forward-travelling wave with $0 < \lambda < 1$ is not sufficiently fast to suppress that growth, thereby making the destabilization still inevitable. $\lambda = 0$ also leads the system to be unstable because there is no way to relax the interface growth. For $\lambda < 0$ the interface wave travels backwards and works coherently with the Marangoni-induced growth, hence reinforcing the destabilization.

If an imbalance arises from the η_x term of the surface velocity in (6), a similar reasoning could lead to instability. As in Wei (2005*a*), this scenario can occur when the air–liquid interface is affected by an additional wind shear τ_s. This interfacial shear τ_s can be in the direction of assisting ($\tau_s > 0$) or opposing ($\tau_s < 0$) gravity-driven base flow. For such a system in a moving frame: $x \to x - (1 + \tau_s)t$, equation (5) remains unchanged, and (6) now becomes

$$\Gamma_t + (\tau_s + 2)\eta_x - M\Gamma_{xx} = 0. \tag{11}$$

A normal-mode analysis reveals that an instability occurs when $\tau_s > 0$ or $\tau_x < -2$, as shown by Wei (2005*a*). When $\tau_s > 0$, it suggests that applying a minute interfacial shear in favour of gravity-driven flow can initiate the Marangoni instability. This is because the applied shear amplifies perturbations to the surfactant concentration, which expedites the Marangoni interface growth. For $\tau_s < 0$, on the other hand, if the shear strength $|\tau_s|$ is weak, the imposed shear being against gravity could weaken the ability to trigger the Marangoni interface growth. But if $|\tau_s|$ is sufficiently large, i.e. $|\tau_s| > 2$, the shear dominates the gravity force; it again suffices to activate the Marangoni instability.

Alternatively, the effect of imposed shear on stability can be elucidated by the concept of vorticity. For the first mode $s = k^2 M\tau_s/2$, $\hat{\Gamma} = -(2\mathrm{i}/(kM) + \tau_s)\hat{\eta}$ and $\hat{\omega} = -\mathrm{i}kM\tau_s\hat{\eta}$. Recall that in the earlier discussion about free falling flow the base-flow-induced Marangoni flow creates in-phase vorticity with the interface deflection, offsetting the out-of-phase vorticity created by perturbations to the basic shear stress. Imposing an additional shear $\tau_s > 0$ tends to make Γ out of phase with η. This effect, through the Marangoni stress $M\Gamma_x$ of (7), makes vorticity lead the interface deflection by $\pi/2$, thereby leading to destabilization. A similar reasoning for $\tau_s < 0$ leads vorticity to lag behind the interface, hence it is stabilizing.

The second mode $s = -\mathrm{i}k - k^2 M(\tau_s + 2)/2$ has $\hat{\Gamma} = (\tau_s + 2)\hat{\eta}$ and $\hat{\omega} = (-2 + \mathrm{i}kM(\tau_s + 2))\hat{\eta}$. In the case of free falling flow ($\tau_s = 0$), this mode is stabilizing as in WJ. The reason is that the induced surfactant concentration (that leads the interface by $\pi/2$ for the first mode) is over-relaxed by the Marangoni diffusion. This tends to make Γ in phase with η. This tendency is further reinforced by a Marangoni flow that acts to decrease the interface deflection for such an in-phase configuration. The resulting vorticity lags behind the interface deflection by $\pi/2$, thus making the system stabilized. When imposing an additional shear on the interface, $\tau_s > 0$ enhances the Marangoni recoil, and the system thus remains stable. For $\tau_s < 0$, if the applied shear is not strong enough to oppose gravity, the system is expected to be stable as above. However, if the applied shear is sufficiently strong against gravity, the corresponding $\Gamma - \eta$ phase configuration will be the reverse; that is, Γ will be out of phase with η, so that vorticity will be ahead of the interface deflection, thereby destabilizing the system.

In the light of the respective effects of the η_x terms on the kinematic condition (10) and surfactant transport (11) shown above, we now combine (10) and (11) (more precisely, written in a fixed frame), and find that instability occurs when $\tau_s + 2 > \lambda + |\lambda|$ or $\tau_s + 2 < \lambda - |\lambda|$, which is equivalent to the following instability threshold:

$$\mathrm{sign}(\tau_s + 2)\left(\tfrac{1}{2}(\tau_s + 2) - \lambda\right) > 0. \tag{12}$$

This instability condition suggests that the instability depends on the combination of two factors: $(\tau_s + 2)$ and $(\tau_s + 2)/2 - \lambda$. The first, $(\tau_s + 2)$, comes from the surface convection η_x term of (11) due to the base flow, and is necessary for instability as suggested by (12). If $\tau_s + 2$ vanishes, the base flow has no influence on rearranging the surfactant distribution; any concentration variation is simply smoothed out by

the Marangoni diffusion, thus no instability occurs. The second, $(\tau_s+2)/2-\lambda$, can be recognized as the difference between cross-products of the coefficients of the η_x and Γ_{xx} terms in (10) and (11). More precisely, if the base flow is capable of re-distributing surfactant, i.e. $\tau_s+2\neq 0$, the onset of instability is determined by whether the flow-induced Marangoni interface growth is stronger than the reducing effects that combine interface-wave travelling and the Marangoni diffusion. In terms of strengths of these effects, the condition of instability requires that the coefficient product of η_x in (11) and Γ_{xx} in (10), $(\tau_s+2)\frac{1}{2}M$, is greater than that of η_x in (10) and Γ_{xx} in (11), λM. Applying (12) with $\tau_s=0$ and $\lambda=1$ (cf. (5) and (6)), we find that the left-hand side of (12) is zero, thereby verifying that there is no occurrence of instability, in line with the observations of the initial value problem shown earlier. As such, a criterion for inception of the surface-shear-mediated Marangoni destabilization can be now established.

3. Two-layer Couette flow with surfactant

3.1. *Problem formulation*

The above section focuses on single-layer flow systems. We now extend the ideas to two-fluid Couette flow systems. Consider two immiscible liquid layers flowing in a channel while undergoing a shear action exerted by two parallel plates, see figure 1(*b*). The bottom layer is occupied by fluid 1 of viscosity μ_1^* and thickness d_1^*. It is overlaid by the second fluid of viscosity μ_2^* and thickness d_2^*. Densities of both fluids are matched and denoted by ρ^*. The fluid–fluid interface contains insoluble surfactant. As in the previous section, we again assume that both gravity and inertial effects are neglected in the problem. As in FH, it is more convenient to analyse the system in a frame moving with the steady-state interfacial velocity. With respect to the interface, the bottom plate moves with a speed of U_w^*, and the top with speed $(d_2^*/d_1^*)\ \mu_1^*U_w^*/\mu_2^*$ in the opposite direction. The characteristic length and velocity are chosen as d_1^* and U_w^*, respectively. The scale of the pressure is $\mu_1^*U_w^*/d_1^*$ and time is scaled by d_1^*/U_w^*. Flow quantities are defined in a way similar to the previous section, as are the interfacial properties. In the dimensionless form, defining the viscosity ratio $m=\mu_2^*/\mu_1^*$ and the depth ratio $d=d_2^*/d_1^*$ $(\geqslant 1)$, the base flows are given by $U_1=y$ for $-1\leqslant y\leqslant 0$, and $U_2=y/m$ for $0\leqslant y\leqslant d$. For long-wavelength perturbations, the governing equations for each fluid are still (1) and (2). The perturbation flow system is subject to the following boundary conditions. The no-slip walls require

$$u_1=v_1=0 \text{ at } y=-1, \quad u_2=v_2=0 \text{ at } y=d. \tag{13}$$

The continuity of velocities across the interface demands

$$u_1=u_2+\left(\frac{1}{m}-1\right)\eta \text{ at } y=0, \tag{14}$$

$$v_1=v_2=0 \text{ at } y=0. \tag{15}$$

The tangential stress condition at the interface is

$$mu_{2y}-u_{1y}=M\Gamma_x \text{ at } y=0. \tag{16}$$

The normal stress condition at the interface reduces to

$$p_1=p_2 \text{ at } y=0. \tag{17}$$

We again neglect surface-tension stabilizing effects in (17) provided the capillary number $Ca = \mu_1^* U_w^*/\sigma_0^* \gg O(k^2)$. Since $p_y = 0$ from the y-momentum equation, $p = p(x)$, hence $p_1 = p_2 = p(x)$ in view of (17). Solving (2) for u of each fluid yields

$$u_1 = \tfrac{1}{2} p_x(y^2 - 1) + A_1(y + 1), \quad u_2 = \frac{1}{2m} p_x(y^2 - d^2) + A_2(y - d), \tag{18}$$

which satisfy (13). Then v can be obtained by continuity accordingly. A_1 and A_2 are undetermined coefficients that depend on η and Γ. Applying the remaining boundary conditions, these coefficients together with p_x can be obtained as follows:

$$p_x = \alpha\eta + \beta M\Gamma_x, \quad A_1 = \alpha_1\eta + \beta_1 M\Gamma_x, \quad A_2 = m^{-1}(\alpha_1\eta + (\beta_1 + 1)M\Gamma_x), \tag{19}$$

where α, β, α_1, and β_1 are auxiliary coefficients:

$$\alpha = 6(1-m)(m-d^2)/\Delta, \quad \beta = -6md(1+d)/\Delta,$$
$$\alpha_1 = \frac{4}{\Delta}(1-m)(m+d^3), \quad \beta_1 = -\frac{1}{\Delta}((3d^2+4d)m + d^4),$$
$$\Delta = m^2 + (4d^3 + 6d^2 + 4d)\,m + d^4.$$

As shown above, α and α_1 reflect viscosity stratification effects; β and β_1 are associated with Marangoni effects. The resulting kinematic and surfactant transport equations become

$$\eta_t + \hat{\alpha}_1\eta_x - \hat{\beta}_1 M\Gamma_{xx} = 0, \tag{20}$$
$$\Gamma_t + \hat{\alpha}_2\eta_x - \hat{\beta}_2 M\Gamma_{xx} = 0, \tag{21}$$

where the coefficients are given by

$$\hat{\alpha}_1 = \frac{\alpha_1}{2} - \frac{\alpha}{3} = \frac{2}{\Delta}(1-m)(d^3+d^2), \quad \hat{\beta}_1 = \frac{\beta}{3} - \frac{\beta_1}{2} = \frac{d^2}{2\Delta}(d^2 - m),$$
$$\hat{\alpha}_2 = 1 + \alpha_1 - \frac{\alpha}{2} = \frac{1}{\Delta}(d+1)((3d+1)\,m + d^3 + 3d^2), \quad \hat{\beta}_2 = \frac{\beta}{2} - \beta_1 = \frac{d}{\Delta}(m + d^3).$$

The above results are equivalent to those obtained by FH. In comparison with FH, however, (20) and (21) are more advantageous for identifying the mechanisms of instability; the insights gained from them can complement the study of FH. Note that the Marangoni parts $\hat{\beta}_1$ and $\hat{\beta}_2$ do not involve contributions from the base flow. Further note that the signs of $\hat{\alpha}_1$ and $\hat{\beta}_2$ depend on $1 - m$ and $d^2 - m$, respectively, and that both $\hat{\alpha}_2$ and $\hat{\beta}_2$ are positive numbers. In comparison with (5) and (6) for falling film flow, these equations have very similar forms at first glance. Although both falling film and two-layer systems have different base flows, they seem to have similar effects on the stability. However, as we have discussed in the foregoing section, the key to instability lies in the detailed way that a base flow rearranges the surfactant distribution and affects the interfacial dynamics. Below we demonstrate the features of (20) and (21).

3.2. *The case of* $m = 1$

We first consider a special case in which viscosities of both fluids are matched ($m = 1$). In this case $\hat{\alpha}_1 = 0$, equations (20) and (21) are reduced to

$$\eta_t - \hat{\beta}_1 M\Gamma_{xx} = 0, \tag{22}$$
$$\Gamma_t + \eta_x - \hat{\beta}_2 M\Gamma_{xx} = 0. \tag{23}$$

Here $\hat{\beta}_1 > 0$. Equation (22) does not have the travelling-wave term η_x due to the absence of viscosity stratification while (23) still preserves the η_x term derived from

the basic shear flow. The instability threshold of (22) and (23) is identified to be $\hat{\beta}_1 > 0$. Since this condition is automatically satisfied, the system is always unstable due to surfactant. This can be also seen by the normal-mode growth rates:

$$s = \pm\frac{1+\mathrm{i}}{2}k^{3/2}M^{1/2}\left(\frac{d^2(d-1)}{(d+1)^3}\right)^{1/2} \tag{24}$$

in which the positive mode is always unstable. Equation (24) agrees with FH. These growth rates vary with $k^{3/2}M^{1/2}$. They can be obtained by retaining only the leading-order terms in each equation, i.e. by neglecting the Marangoni diffusion term $\hat{\beta}_2 M\Gamma_{xx}$ in (23). Physically, as we shall also show later for an initial value problem, since the Marangoni-induced interface growth is reduced neither by the travelling-wave depletion nor by the Marangoni diffusion, the interface deflection amplifies without being restored, leading the system to be unstable. Wei & Rumschitzki (2005) and Wei (2005*b*) asymptotically examined the stability of surfactant-laden core–annular film flows. In their studies, for weak interfacial tensions, similar sets of evolution equations and growth rates were also found in the absence of viscosity stratification. This is expected because for weak tensions the capillary effect due to the cylindrical interface does not contribute to the instability; the problem is identical to that in a planar system.

Note that the $O(k^{3/2})$ growth rates found in (24) cannot be simply obtained by using the standard Yih expansion technique unless one can identify the appropriate expansion in k. In fact, the scale of the growth rates can be identified using the following scaling argument. Letting the time scale be T, (22) and (23) suggest $\eta/T \sim k^2 M\Gamma$ and $\Gamma/T \sim k\eta$, respectively. These scalings yield $T \sim k^{-3/2}M^{-1/2}$ and $\Gamma \sim k^{-1/2}M^{-1/2}\eta$. The inverse of the former just gives the growth rate scale shown above. The latter implies that the perturbation to the surfactant concentration is large compared to that to the interface.

We now employ the vorticity argument to illustrate the instability for the $m = 1$ system (cf. (22) and (23)). There are some aspects worth addressing concerning differences between two-layer and free-surface flows. As discussed in the preceding section, the vorticity generated in free-surface flow can be directly related to the velocity normal to the unperturbed interface. This is the vorticity causing the interface to grow or decay. It is based on the fact that perturbation flow is linear (cf. (4)) and vorticity remains uniform across the layer (cf. (7)). However, for a two-layer flow in a channel, as pointed out by Charru & Hinch (2000), perturbation flows need to fulfil the requirement of no net flow across the channel (mass conservation); linear perturbation flows as in a single-layer system generally do not satisfy that condition. This requires the development of pressure perturbations. Hence, vorticity has to be mediated by pressure as indicated by (18). More precisely, due to mass conservation, the vorticities of both fluids at the interface can be related to the pressure gradient, which is shown as follows. Define the perturbation flow rate in the x-direction for each layer:

$$Q_1 = \int_{-1}^{0} u_1\,\mathrm{d}y \quad \text{and} \quad Q_2 = \int_{0}^{d} u_2\,\mathrm{d}y.$$

With the aid of $A_i = -\omega(y=0)\,(i=1,2)$ in (18), these flow rates can be written as

$$Q_1 = -\frac{p_x}{3} - \frac{1}{2}\omega_1(y=0) \quad \text{and} \quad Q_2 = -\frac{p_x}{3m}d^3 - \frac{d^2}{2}\omega_2(y=0).$$

Mass conservation demands $Q_1 + Q_2 = 0$, thus leading to

$$\frac{1}{2}(\omega_2 d^2 - \omega_1)_{y=0} = \frac{1}{3} p_x \left(1 + \frac{d^3}{m}\right).$$

Replacing p_x in terms of the two vorticities, the flow rate of the bottom layer can be expressed in the form

$$Q_1 = \frac{-md^2}{2(m + d^3)} \left(\frac{d}{m}\omega_1 + \omega_2\right)_{y=0}, \tag{25}$$

which determines the growth rates through the kinematic condition $Q_{1x} + \eta_t = 0$. Since $(-m\omega_2 + \omega_1)_{y=0} = M\Gamma_x$ in view of (16), $\omega_1(y = 0)$ and $\omega_2(y = 0)$ are generally not in phase when surfactant is present. Hence the stability/instability depends on competition between vorticities of layers. Equation (25) suggests that the larger d, the more dominant the bottom-layer vorticity becomes since large d weakens the top-layer flow. On the other hand, large m makes the top-layer vorticity more dominant because the interface sees the more viscous top layer as a rigid wall that serves a source of generating vorticity.

For $m = 1$, inspecting (18) and (19) reveals that $\alpha = \alpha_1 = 0$, so perturbation vorticity is generated only by Marangoni stresses without being regulated by the interface deflection. At the interface, the vorticity of each fluid is

$$\omega_1(y = 0) = -\beta_1 M\Gamma_x(\beta_1 < 0) \quad \text{and} \quad \omega_2(y = 0) = -\beta_2 M\Gamma_x(\beta_2 = \beta_1 + 1 > 0).$$

When $d > 1$, since the magnitude of $d\omega_1(y = 0)$ is larger than that of $\omega_2(y = 0)$, the bottom-layer vorticity dominates the dynamics. Inspecting the eigenfunctions, we find $\hat{\Gamma} = \mp(1 + \mathrm{i})(d^2(d - 1)(d + 1)^{-3})^{-1/2}k^{-1/2}M^{-1/2}\hat{\eta}$ corresponding to the positive and negative modes of (24), respectively. The associated normal-mode vorticity of the bottom layer is $\hat{\omega}_1 = \pm(1 - \mathrm{i})(d^2(d - 1)(d + 1)^{-3})^{-1/2}|\beta_1|k^{1/2}M^{1/2}\hat{\eta}$. Note that in (24) for $d > 1$ the positive (negative) mode has $s_i > 0\,(<0)$, indicating backward (forward) propagation of the interface. For the positive mode, since Γ lags behind η by $3\pi/4$, the induced vorticity lags behind the interface by $\pi/4$ and in turn gives rise to destabilization. A similar reasoning for the negative mode leads to stabilization.

Like our explanation above, FH applied the phase difference between Γ and η to illustrate stability/instability by considering the $m = 1$ case with a much thicker upper layer ($d \gg 1$). Since the $\Gamma-\eta$ phase difference for the positive (negative) mode is $5\pi/4$ ($\pi/4$), it can be viewed as being close to out of phase (in phase), leading to an unstable (a stable) result as a consequence of the actions of Marangoni forces on the deflected interface. The $m = 1$ system lacks reducing effects at leading order in k; the Marangoni force is thus the sole effect responsible for the system stability. As indicated by (20) and (21), for $m \neq 1$ since reducing effects are generally involved, Γ and η are neither close to out of phase nor in phase. Applying only the Marangoni argument cannot explain general features of stability. As we shall discuss later for $m \neq 1$, the stability features can be better explained by the vorticity-based argument. In fact, appropriate interpretations using the $\Gamma-\eta$ phase difference should be based on evolution equations with the aid of initial-value-problem observations.

We now conduct an initial value simulation of (22) and (23) to examine the associated instability mechanisms. Given an initial sinusoidal perturbation of the interface, figure 6 shows the spatio-temporal evolutions for both η and Γ. In the early stages of the evolution, the surfactant perturbation grows very rapidly while the interface virtually remains still. The stillness of the interface is attributed to the lack of

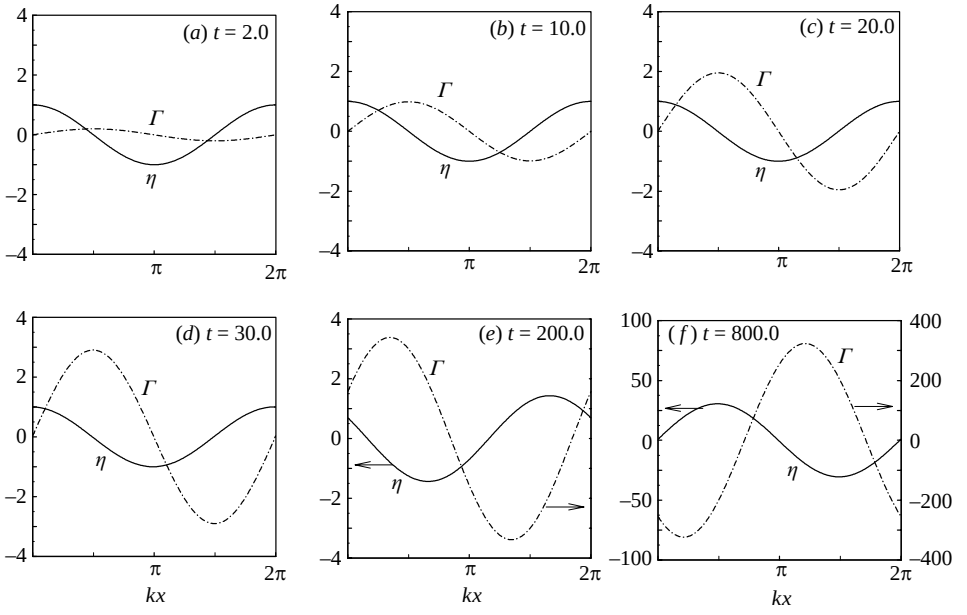

FIGURE 6. The spatio-temporal evolution of η and Γ for a two-fluid Couette flow. $m=1$, $d=2$, $M=1$. $k=0.1$. In (*e*) and (*f*), the scale for Γ is shown on the right vertical axes. Arrows are used for referring to the axes, and do not indicate motions.

the travelling term η_x in (22). With such an interface the surfactant concentration perturbation amplifies linearly with time (figure 6*b–d*) according to $\Gamma \sim -\eta_x(t=0)t$ (cf. $\Gamma_t+\eta_x=0$, equation (23) with negligible Marangoni term). We also verify that the early-stage ($t<30$) evolutions of Γ do not depend on d, confirming that the initial amplification of Γ is solely derived from the base-flow-induced surface velocity. Compared to figure 3, we find that the early-time growth of Γ is relatively slower than that of falling film flow. This is because the coefficient of the base-flow term η_x of (23) is half of that of (6) of falling film flow. These early-stage evolutions suggest that although the types of base flows are different, they produce the same effects of amplifying the surfactant concentration variations. Even though a falling film flow has a faster early growth in Γ than a two-layer $m=1$ Couette flow, whether such a growth can persist so as to determine the fate of a system lies in the reducing effects. A falling film flow has reducing effects that can make the growth decay at later times while a two-layer $m=1$ Couette flow does not. This key difference cannot be identified by the eigenfunction analysis; rather, the initial value approach can provide more insight into all occurrences at different time scales in the course of the evolution.

In the later stages of the evolution (figure 6*e*, *f*), the surfactant perturbation grows very rapidly compared to the interface. The instability is mainly attributed to the lack of the η_x term in (22) in providing travelling-wave suppression upon the flow-induced Marangoni interface growth. In addition, since $M\Gamma_{xx}$ is a higher order effect than η_x in (23), the surfactant concentration perturbation can be further magnified by the growing interface without being recoiled by the Marangoni diffusion, which exaggerates the destabilizing effect on the system. Figure 7 shows the temporal evolution of the amplitudes of η, Γ and ω_1. The vorticity ω here is chosen as the bottom-layer one ω_1 since it dominates the dynamics for $d>1$ and $m=1$. Initial growth (for

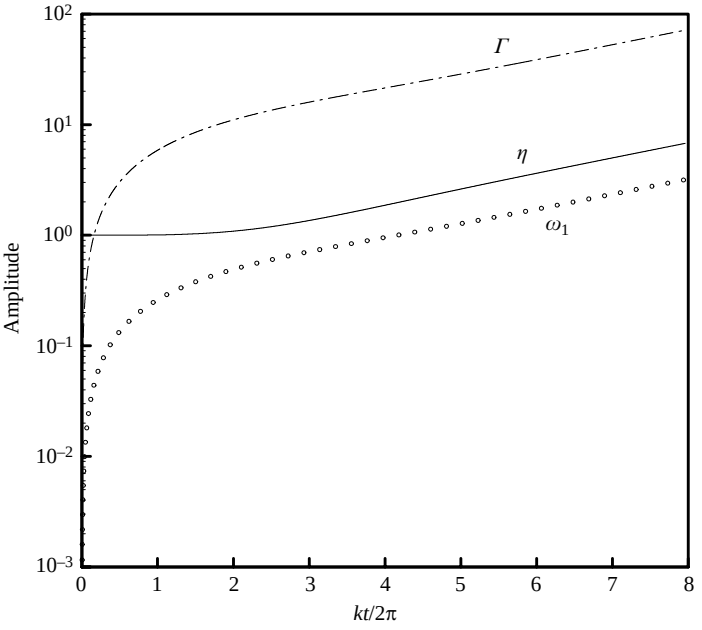

FIGURE 7. The temporal evolution of the amplitudes of η, Γ and ω_1 corresponding to figure 6.

$kt/2\pi < 2.5$) of both Γ and ω_1 is much faster than that of η. Long-term behaviours of η and Γ qualitatively confirm $\Gamma \sim k^{-1/2} M\eta$ shown earlier using a scaling argument. In addition, in comparison with figure 4 for falling film flow, the amplitudes grow monotonically with time without oscillation. This is because oscillation is an indication of the participation of reducing effects arising from travelling waves, and travelling waves are absent for $m = 1$ here.

Figure 8 shows the evolution of $\Gamma - \eta$ and $\omega_1 - \eta$ phase differences. Initially, similar to the falling film case, Γ has a phase difference of $-\pi/2$ with η owing to the base-flow-excited surfactant perturbation (cf. $\Gamma_t = -\eta_x$). The developed Marangoni stress retards η, enlarging the phase difference with Γ. The long-time $\Gamma - \eta$ phase difference approaches $-3\pi/4$, which is consistent with the eigenfunction result. Since ω_1 is directly related to the Marangoni stress $M\Gamma_x$, it shifts the $\Gamma - \eta$ phase by $\pi/2$ and makes ω_1 lag behind η by $\pi/4$, thereby leading the system to instability

3.3. *The case of* $m \neq 1$

When there is viscosity stratification ($m \neq 1$), in contrast to $m = 1$, it activates the travelling-wave term $\hat{\alpha}_1 \eta_x$ in (20). Since $\hat{\alpha}_1$ is proportional to $1 - m$, the interface travel forwards (backwards) for $m < 1\,(>1)$. Because the interface evolution also can be determined by the Marangoni term $\hat{\beta}_1 M \Gamma_{xx}$ in (20), it is important to know how Marangoni forces act, depending on the sign of $\hat{\beta}_1$, i.e. $(d^2 - m)$. When a Marangoni stress is exerted on the fluid–fluid interface, its drag is more effective for a more viscous fluid. When one fluid flows in one direction, the other flows oppositely as a consequence of mass conservation. Since the interface response depends on the contrast in velocities between two fluids, this is further affected by the depth of each fluid. If the top layer has a sufficiently large depth, its motion is slow; the response of the interface to Marangoni forces is mainly controlled by the bottom-layer motions. But the response can be reversed when the top fluid has a sufficiently high viscosity.

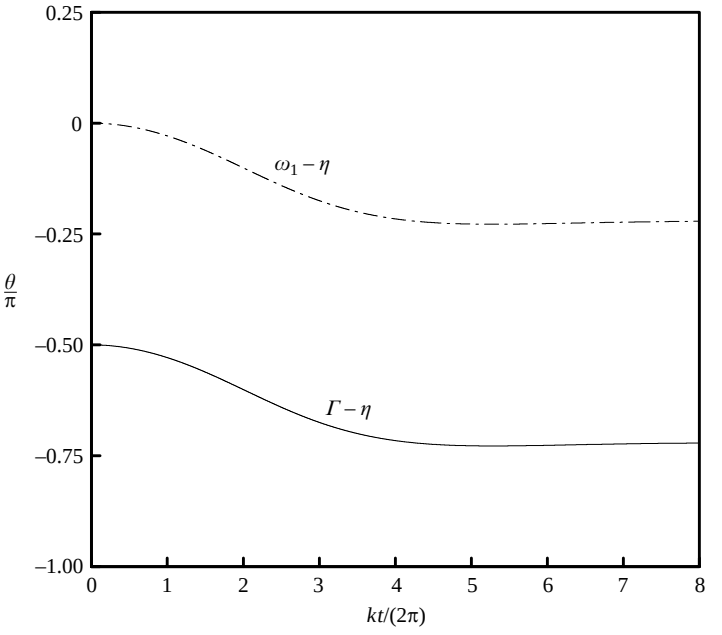

FIGURE 8. The temporal evolution of the phase differences $\Gamma - \eta$ and $\omega_1 - \eta$ corresponding to figure 6.

This also can be verified by the following argument. The Marangoni-induced linear velocity profiles require $u_1 \sim u_2 d$ to fulfil the zero-net-flow constraint. The tangential stress at the interface (16) requires $\sigma_x = u_{1y} - m u_{2y} \sim (d^2 - m)u_1/d$. This explains why the competing effects of viscosity and depth on the Marangoni actions are reflected by $(d^2 - m)$ in $\hat{\beta}_1$. A similar argument was given previously by Charru & Hinch (2000) for a clean-interface two-layer system.

Equation (20) reveals that for $d^2 > m$ ($d^2 < m$) the interfacial response to Marangoni flows is reflected by the bottom (top) fluid motion. It follows that a perturbation to the surfactant concentration tends to cause the induced interfacial displacement to be out of phase (in phase) with it. It also implies that if instability occurs in the system, increasing the top-layer viscosity can eventually suppress the instability and stabilize the system. Such a Marangoni effect associated with viscosity stratification was previously found by FH, and also identified numerically by BP. We provide an explanation here. Therefore for a given depth d, there is a critical viscosity ratio m at which the above-mentioned effects of viscosity and depth cancel out exactly. In this situation ($\hat{\beta}_1 = 0$) Marangoni flows have no impacts on the interfacial evolution; the interface just continues to travel without any change in its amplitude, therefore no instability occurs. The same critical condition found by FH for the onset of instability can be now explained.

In short, viscosity stratification can influence the interfacial dynamics so that it can alter the outcome of the system stability. As indicated by (20), the effects of viscosity stratification are twofold. On the one hand, it either affects the speed of an interfacial wave or changes the wave propagating direction; on the other hand, it modifies how the interfacial material responds to Marangoni forces. According to (21), since an interfacial perturbation also can affect the surfactant concentration through the surface advection along the interface, how the induced Marangoni flow acts with

respect to the prevailing travelling motion of the interface through (20) determines the subsequent interfacial development, and hence the stability. Below we illuminate all occurrences for $m \neq 1$ in more detail.

For $m \neq 1$, we first inspect the normal-mode growth rates of (20) and (21), and then discuss the associated instability mechanisms. These growth rates are given by

$$s = \frac{(1-d)}{4(m-1)} Mk^2, \tag{26}$$

$$s = \frac{2\mathrm{i}(m-1)(d^3+d^2)}{\Delta} k + \frac{(d^2-m)((3d+1)m+d^3+d^2)}{4(m-1)\Delta} Mk^2, \tag{27}$$

which agree with FH. Similar growth rate expressions for surfactant-laden core–annular flows were also found in the low-tension limit (Wei 2005*b*). For $d \geqslant 1$, when $m < 1$, the first mode is unstable while the second is stable. When $m > 1$, the first mode becomes stabilizing; the system can be destabilized by the second mode if $d^2 > m$. Thus, instability occurs when $d^2 > m$ as in FH, verifying the earlier discussion about the instability criteria based on Marangoni actions. This also suggests that the parameters $\hat{\alpha}_1$ (containing $1-m$) and $\hat{\beta}_1$ (containing d^2-m) in (20) play key roles in determining the onset of instability.

We now apply vorticity arguments to illustrate stability/instability for $m \neq 1$. The eigenfunction is given by $\hat{\Gamma} = -(s + \mathrm{i}\hat{\alpha}_1 k)\hat{\beta}_1^{-1} k^{-2} M^{-1} \hat{\eta}$ from (20). The normal-mode vorticity at the interface for each fluid is $\hat{\omega}_1(y=0) = -\alpha_1 \hat{\eta} - \mathrm{i}\beta_1 kM\hat{\Gamma}$ and $\hat{\omega}_2(y=0) = m^{-1}(-\alpha_1 \hat{\eta} - \mathrm{i}(\beta_1+1)kM\hat{\Gamma})$. As revealed by (25), since instability depends on both $d\hat{\omega}_1(y=0)/m$ and $\hat{\omega}_2(y=0)$, their competition determines the instability. To illustrate how these vorticities determine the system's stability, below we consider two limiting cases: (i) the large-gap limit $d \gg 1$ with moderate viscosity contrast $m = O(1)$, and (ii) the large-m limit with $d = O(1)$.

In the large-gap limit $d \gg 1$, $|\alpha/\alpha_1| \ll 1$ and $|\beta/\beta_1| \ll 1$; the flow adjusted by altered pressure can be considered to be relatively weak compared to linear flows in view of (19). In this case, $\hat{\alpha}_1 \sim \alpha_1/2 \sim 2(1-m)/d$ and $\hat{\beta}_1 \sim \beta_1/2 \sim 1/2$, hence $\hat{\Gamma} \sim -(2s + \mathrm{i}\alpha_1 k)\beta_1^{-1} k^{-2} M^{-1} \hat{\eta}$. This leads to $\hat{\omega}_1(y=0) \sim -2\mathrm{i}k^{-1} s\hat{\eta}$ and $\hat{\omega}_2(y=0) \sim O(d^{-1})$, suggesting that the bottom layer dominates the dynamics. This is expected since the top layer has much weaker flow than the bottom one when d is large. For $m > 1$, the first mode $s \sim -dMk^2/4(m-1)$ makes the bottom-layer vorticity lag behind the interface by $\pi/2$, and thus is stabilizing. The second mode $s \sim Mk^2/4(m-1)$ just does the opposite. Similarly, $m < 1$ reverses the above trends.

For the case of $m \gg 1$ with $d = O(1)$, $\hat{\alpha}_1 \sim -2(d^3+d^2)/m$, $\hat{\beta}_1 \sim -d^2/(2m)$, $\alpha_1 \sim -4$ and $\beta_1 \sim -(3d^2+4d)/m$. We have

$$\hat{\Gamma} \sim 2md^{-2}(s - 2\mathrm{i}(d^3+d^2)m^{-1}k)k^{-2}M^{-1}\hat{\eta}, \hat{\omega}_1(y=0)$$
$$\sim m^{-1}(4m\hat{\eta} + \mathrm{i}(3d^2+4d)kM\hat{\Gamma}) \quad \text{and} \quad \hat{\omega}_2(y=0) \sim m^{-1}(4\hat{\eta} - \mathrm{i}kM\hat{\Gamma}).$$

In this limit, the first mode $s \sim (1-d)Mk^2m^{-1}/4$ yields

$$\hat{\omega}_1(y=0) \sim (4 + 4(d+1)(3d^2+4d)m^{-1})\hat{\eta} \quad \text{and} \quad \hat{\omega}_2(y=0) \sim (4 - 4(d+1))m^{-1}\hat{\eta}.$$

Since vorticity is either in phase or out of phase with the interface, no instability occurs. Similarly, the second mode $s \sim 2\mathrm{i}m^{-1}(d^3+d^2)k - (3d+1)m^{-1}Mk^2/4$ does not lead to instability since both vorticities are in phase with the interface in view of

$$\hat{\omega}_1(y=0) \sim (4 + O(m^{-1}k))\hat{\eta} \quad \text{and} \quad \hat{\omega}_2(y=0) \sim (4 + O(k))m^{-1}\hat{\eta}.$$

Physically, for $m \gg 1$ the bottom layer sees the interface as a rigid surface; this tends to damp perturbations, hence leading to a stable system.

As shown above, when both d and m are large, the first mode is stabilizing, but the second mode can be either destabilizing or stabilizing because of $(d^2 - m)$ in (27). To understand the competition between large d and m effects from the vorticity viewpoint, we let $m = \tilde{m}d^2$ with $d \gg 1$ and $\tilde{m} = O(1)$. The second mode becomes

$$s \sim \mathrm{i}k/2 + (1 - \tilde{m})(3\tilde{m} + 1)\tilde{m}^{-2}d^{-2}Mk^2/16.$$

The vorticities are

$$\hat{\omega}_1(y = 0) \sim (1 - \mathrm{i}kM\tilde{m}^{-2}d^{-2}(3\tilde{m} + 1)^2/8)\hat{\eta} \quad \text{and}$$
$$\hat{\omega}_2(y = 0) \sim \tilde{m}^{-1}d^{-2}(1 + \mathrm{i}kM\tilde{m}^{-1}d^{-1}(3\tilde{m} + 1)/2)\hat{\eta}.$$

Noticing that $s_i > 0$ here, the bottom-layer vorticity lags behind the interface and is destabilizing while the top-layer vorticity is stabilizing. Since (25) reveals that

$$\hat{\Omega} \equiv (d\hat{\omega}_1/m + \hat{\omega}_2)_{y=0} \sim (\tilde{m}^{-1}(d^{-1} + d^{-2}) - 3\mathrm{i}k^{-1}\tilde{m}^{-3}d^{-3}(3\tilde{m} + 1)(\tilde{m} - 1)/8)\hat{\eta},$$

instability thus occurs when $\tilde{m} < 1$ or $m < d^2$. For large d and $d^2 > m$ the instability can be understood by the fact that the destabilization due to the bottom layer becomes more dominant than the stabilization due to the top layer. The dominance of the bottom layer here can also be identified by the earlier scaling argument using both mass conservation and the tangential stress condition.

In fact, the instability threshold $m = d^2$ can be obtained through the vorticity argument as follows. One can show that

$$\hat{\Omega} = (d^3 + m)m^{-1}\Delta^{-1}[4(d + 1)(m - 1)\hat{\eta} - \mathrm{i}k(m - d^2)M\hat{\Gamma}].$$

It thus becomes clear that $m = d^2$ makes Ω in phase or out of phase with η, and does not lead to any instability. Instability demands the phase difference between $\hat{\Gamma}$ and $\hat{\eta}$ to differ from $\pi/2$; the $\Omega - \eta$ phase difference and hence instability are determined by the sign and magnitude of $(m - d^2)$. For the second mode (27), we find

$$\hat{\Omega} = (d^3+m)m^{-1}\Delta^{-1}[4(d+1)(m-1)+\mathrm{i}kM(m-d^2)((3d^{-1}+d^{-2})m+d+1)(m-1)^{-1}/2]\hat{\eta}.$$

Therefore for $m > 1$ it becomes evident that the occurrence of instability requires $m < d^2$ by setting the overall vorticity to lag behind the interface in view of $s_i > 0$.

An alternative way to find the instability threshold of (20) and (21) is to follow a similar procedure for arriving at (9) for a falling film flow. We find

$$\mathrm{sign}(\hat{\alpha}_2\hat{\beta}_1)(\hat{\alpha}_2\hat{\beta}_1 - \hat{\alpha}_1\hat{\beta}_2) > 0. \tag{28}$$

As a result, the onset of instability depends on both $\hat{\alpha}_2\hat{\beta}_1$ and $\hat{\alpha}_2\hat{\beta}_1 - \hat{\alpha}_1\hat{\beta}_2$. $\hat{\alpha}_2\hat{\beta}_1$ indicates that the base-flow-induced Marangoni effect is necessary for the instability. Its sign, determined by $\hat{\beta}_1$ (via $d^2 - m$), reflects the way the fluids respond to the Marangoni flow. $\hat{\alpha}_2\hat{\beta}_1 - \hat{\alpha}_1\hat{\beta}_2$ results from the competition between Marangoni-triggered interface growth and reducing effects combining the interface travelling and the Marangoni diffusion. Notice that the reducing effects have to be accommodated in the viscosity stratification (reflected by $\hat{\alpha}_1$). For $\hat{\alpha}_1 \neq 0$ (i.e. $m \neq 1$), since $\hat{\alpha}_2\hat{\beta}_1 - \hat{\alpha}_1\hat{\beta}_2 = (d - 1)(d^3 + d^2)/(2\Delta) > 0$ for $d > 1$, the instability threshold is $\hat{\beta}_1 > 0$ or $d^2 > m$ as in FH. For $d = 1$, $\hat{\alpha}_2\hat{\beta}_1 - \hat{\alpha}_1\hat{\beta}_2 = 0$ does not lead to any instability, which is clear because of the reversibility of Stokes flow. When $\hat{\alpha}_1 = 0$ (i.e. $m = 1$), however, no reducing effects mitigate the Marangoni-induced interface growth; the condition (28) is automatically satisfied as long as $d \neq 1$. In this case, instability can persist as shown by (24).

The condition (28) is established provided that surface diffusion is negligible. Surface diffusion clearly enhances reducing effects on the instability. In this case, condition (28) is modified by replacing $\hat{\beta}_2$ with $\hat{\beta}_2 + (Pe_s M)^{-1}$ where $Pe_s = U_w^* d_1^*/D_s^*$ is the surface Péclet number with D_s^* being the surface diffusivity. That is,

$$\text{sign}(\hat{\alpha}_2\hat{\beta}_1)(\hat{\alpha}_2\hat{\beta}_1 - \hat{\alpha}_1\hat{\beta}_2) > \text{sign}(\hat{\alpha}_2\hat{\beta}_1)\hat{\alpha}_1(MPe_s)^{-1}. \tag{29}$$

In comparison with condition (28), condition (29) depends on MPe_s when surface diffusion is present. Note that MPe_s does not depend on velocity, but on surfactant and fluid properties. It is clear that the onset of instability has to overcome additional reducing effects due to surface diffusion. Since $\hat{\alpha}_1$ is positively proportional to $(1-m)$, for $m > 1$ the instability threshold $d^2 > m$ still holds regardless of the presence of surface diffusion. On the other hand, $m < 1$ requires a relatively thick top layer $d > 4(1-m)(MPe_s)^{-1} + 1$ to trigger instability.

To aid in understanding the features of stability for $m \neq 1$, we again inspect the spatio-temporal evolution of (20) and (21). We first consider the case of $m < 1$. In this case, $d^2 > m$, so the Marangoni flow is mainly reacted by the bottom layer. The interface travels forwards with an $O(k)$ wave speed in view of $\hat{\alpha}_1\eta_x$ (with $\hat{\alpha}_1 > 0$). The perturbed interface activates the surfactant concentration variation according to (21). This leads to the induced surfactant concentration having a phase of $\pi/2$ ahead of the interface. At the earlier stages of the evolution, a slow change in the interfacial motion amplifies the surfactant concentration perturbation very rapidly. The induced Marangoni flow, to which the bottom-fluid motion responds, tends to cause an increase (a decrease) in the interface amplitude for the interface portions where $\eta_x < 0$ (> 0). This is the Marangoni effect that tends to induce the interface growth. Since the Marangoni growth is in the direction opposite to that in which the interface travels (i.e. $\hat{\alpha}_1\eta_x$ and $-\hat{\beta}_1\Gamma_{xx}$ are out of phase), the interface growth slows down, as does the steepening process of the surfactant concentration. For $m = 0.5$ and $d = 2$, figure 9 shows the temporal evolution of the amplitudes of η, Γ and ω_i $(i = 1, 2)$. As revealed in figure 9, the early-stage ($kt/2\pi < 3$) interface amplitude decreases slowly with time, indicating that the interface-wave depletion due to $\hat{\alpha}_1\eta_x$ is slightly stronger than the Marangoni growth due to $-\hat{\beta}_1 M\Gamma_{xx}$. Meanwhile, while the surfactant concentration continues to be steepened by the slowly changing interface, the developed Marangoni diffusion is not sufficiently strong to reduce the growing surfactant concentration gradient. As a result, this steepening surfactant concentration accelerates the Marangoni growth; the interface amplitude then starts to increase with time, leading the system to become unstable for long time. For most of time, the top-layer vorticity contribution is greater than the bottom-layer one, thus the top layer dictates the dynamics. This explains why ω_2 almost follows the trend of η while ω_1 does not.

The above results for $m < 1$ combine some features from a falling film (figure 4) and those from the $m = 1$ case (figure 7). The early-time, transitory modulation between reducing effects and the Marangoni growth ($kt/2\pi < 5$) are similar to figure 4 for falling film flow while the long-time behaviours resemble figure 7 for the $m = 1$ case. Figure 10 shows the evolution of phase differences $\Gamma - \eta$, $\omega_1 - \eta$ and $\omega_2 - \eta$. The $\Gamma - \eta$ phase difference decreases with time initially and is then followed by a transitory modulation due to reducing effects. Its long-time value reaches 0.55π which is consistent with the leading-order eigenfunction $\hat{\Gamma} \sim -\mathrm{i}\hat{\alpha}_1\hat{\beta}_1^{-1}k^{-1}M^{-1}\hat{\eta}$ corresponding to the first-mode growth rate ($O(k^2)$) of (26). The phase differences $\omega_1 - \eta$ and $\omega_2 - \eta$ behave differently. The former decreases with time initially and has a negative steady value ($\sim -0.17\pi$ indicating stabilization) while the latter increases initially and its steady value is positive ($\sim 0.97\pi$ indicating destabilization). Note again that $\theta > \pi$

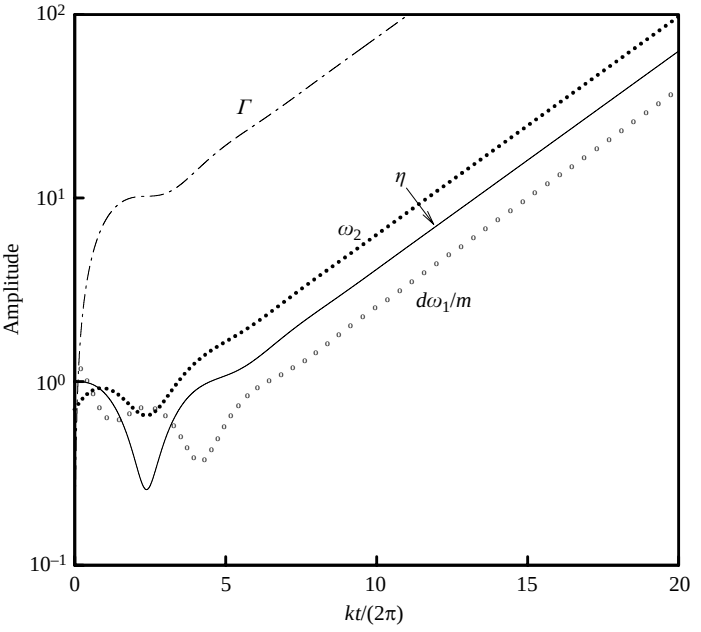

FIGURE 9. The temporal evolution of the amplitudes of η, Γ and ω_i $(i = 1, 2)$ for a two-fluid Couette flow with $m < 1$. $m = 0.5$, $d = 2$, $M = 1$, $k = 0.1$.

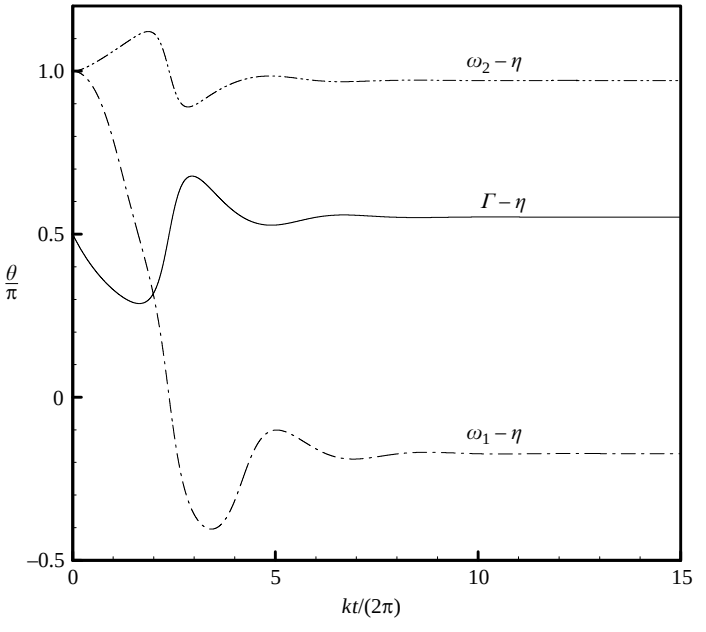

FIGURE 10. The temporal evolution of the phase differences $\Gamma - \eta$ and $\omega_i - \eta$ corresponding to figure 9. Note that a phase θ larger than π should be read as a phase lag of $(2\pi - \theta)$.

should be read as a phase lag of $(2\pi - \theta)$. Since ω_2 dominates the dynamics in view of its larger magnitude than $d\omega_1/m$ shown in figure 9, destabilizing effects due to ω_2 are more important than stabilizing effects due to ω_1. This explains why the $\Gamma - \eta$ phase difference responds closely to the change in the $\omega_2 - \eta$ phase difference. Also, because

of the smaller magnitude of $d\omega_1/m$, the $\omega_1 - \eta$ phase difference takes a longer time than the $\omega_2 - \eta$ one to reach its steady value.

For $m > 1$, in contrast to $m < 1$, $\hat{\alpha}_1 \eta_x$ makes the interface travel backwards. In this situation, two cases $d^2 > m$ and $d^2 < m$ are considered separately. For $d^2 > m$, the results for $d = 2$ with several m are shown in figure 11. As shown in figure 11, the value of $d\omega_1/m$ is larger than that of ω_2, so that the bottom layer controls the dynamics. Further inspection of the $\omega - \eta$ phase differences (not shown) reveals that ω_1 lags behind η while ω_2 leads η. Since ω_1 has destabilizing effects in view of a backward-travelling interface, the system eventually becomes unstable. These results are also consistent with the features due to the second mode of (27). In comparison with the $m < 1$ evolution shown in figure 9, the interface amplitude increases monotonically with time. This is because $\hat{\alpha}_1 \eta_x$ and $-\hat{\beta}_1 \Gamma_{xx}$ are in phase unlike the $m < 1$ case; the backward-travelling interface tends to encourage the Marangoni-induced interface growth although the growth rates are smaller than the $m < 1$ case. Figures 7 and 11 reveal that for $d^2 > m$ the larger m, the longer the transition period. This can be understood by the fact that the more viscous the top layer is, the smaller $\hat{\beta}_1$ in (20), weakening the Marangoni growth and hence making reducing effects last longer.

For $d^2 < m$, however, the flow response to Marangoni effects is switched to the top fluid layer. The Marangoni flow acts in an opposite manner to that of the $d^2 > m$ case. That is, it tends to thin (thicken) the bottom layer at the location where the surfactant concentration is lower (higher). The resulting flow-induced Marangoni effect causes an increase (a decrease) in the interface amplitude for the interface portions where $\eta_x > 0$ (<0), making the interface grow in a forward direction. This growth is relieved by the backward-travelling motion of the interface. Typical amplitude evolution is shown in figure 12. Results show that the bottom layer controls the dynamics because of its greater vorticity contribution than the top layer. We have identified that the evolution is dominated by the first mode whose growth rate is purely real and that ω_1 is shown to lag behind η; the system is thus stable as revealed in figure 12. In contrast to the $d^2 > m$ case, stabilizing effects combining the interface-wave travelling and the Marangoni diffusion now become stronger than the flow-induced Marangoni destabilization. These competing effects dominate alternately in the course of the evolution, but are overall in favour of stabilization in view of the instability criterion (28). Therefore, the flow-induced surfactant concentration perturbation gradually fades away in a time-oscillatory manner, as does the interface amplitude. The evolution is similar to that of the falling film flow system shown in figure 4. A transitory behaviour found by BP also can be explained in a way similar to the above.

4. Extension to the weakly nonlinear regime

In the light of the linear stability analysed so far, we would like to briefly discuss its extension to the weakly nonlinear regime. Here we choose two-layer Couette flow for the case study since it contains all the physical elements determining the stability, as discussed in § 3. The relevant set of weakly nonlinear evolution equations is derived below. We start with the flow rate of each layer by retaining the first-order correction due to the interfacial deflection:

$$Q_1 = \int_{-1}^{\eta} u_1 \, \mathrm{d}y \sim \frac{p_x}{2}\left(-\frac{2}{3} - \eta\right) + A_1\left(\frac{1}{2} + \eta\right), \tag{30a}$$

$$Q_2 = \int_{\eta}^{d} u_2 \, \mathrm{d}y \sim \frac{p_x}{2m}\left(-\frac{2d^3}{3} + d^2\eta\right) + A_2\left(-\frac{d^2}{2} + d\eta\right), \tag{30b}$$

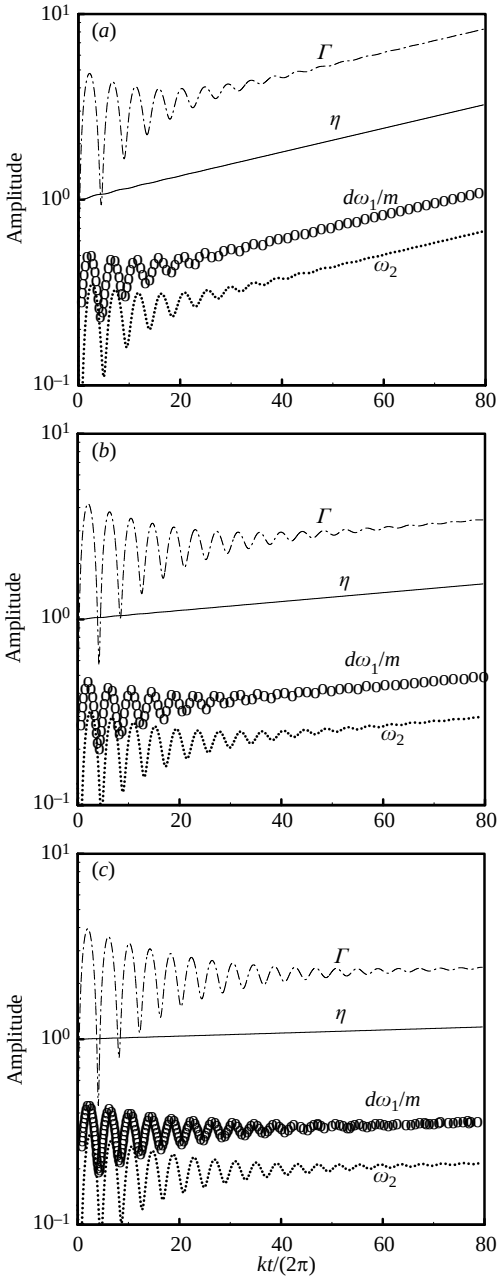

FIGURE 11. The temporal evolution of the amplitudes of η, Γ and ω_i $(i = 1, 2)$ for a two-fluid Couette flow with $m > 1$ and $m < d^2$. $d = 2$, $M = 1$. $k = 0.1$. (*a*) $m = 3$, (*b*) $m = 3.5$, (*c*) $m = 3.8$.

where A_1 and A_2 are solved using (13), (14), (16), and (17), and given by

$$A_1 = \frac{m}{(m+d)}\left[\frac{1}{2}\left(1-\frac{d^2}{m}\right)p_x + \left(\frac{1}{m}-1\right)\eta\right] - \frac{d}{(m+d)}M\Gamma_x,$$

$$A_2 = \frac{1}{(m+d)}\left[\frac{1}{2}\left(1-\frac{d^2}{m}\right)p_x + \left(\frac{1}{m}-1\right)\eta + M\Gamma_x\right].$$

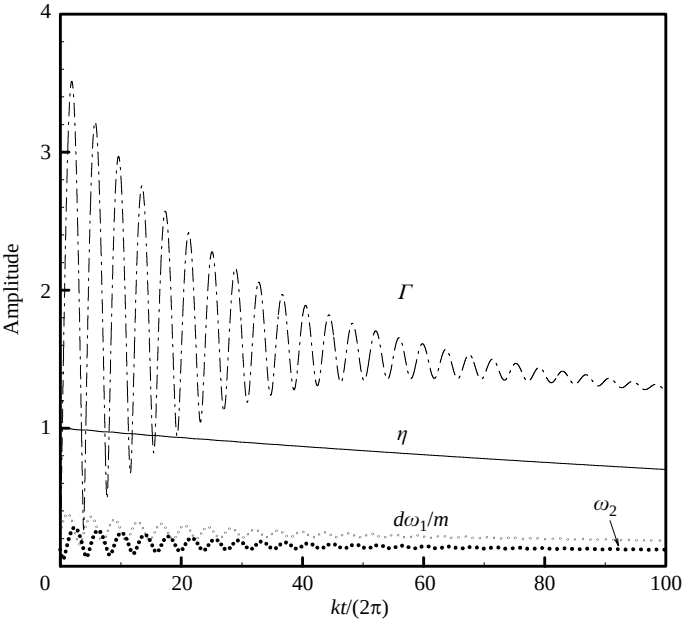

FIGURE 12. The temporal evolution of the amplitudes of η, Γ and ω_i $(i = 1, 2)$ for a two-fluid Couette flow with $m > 1$ and $m > d^2$. $m = 4.5$, $d = 2$, $M = 1$. $k = 0.1$.

The zero-net-flow constraint $Q_1 + Q_2 = 0$ requires the pressure gradient to be adjusted as

$$p_x = \alpha\eta + \beta M\Gamma_x + \gamma\eta^2, \tag{31}$$

with $\gamma = (12/\Delta)(1-m)(m+d)$. Using (31), u_1 in (18) can be obtained in terms of η and Γ_x, and hence Q_1. Applying the kinematic condition $\eta_t + Q_{1x} = 0$ and the surfactant transport equation $\Gamma_t + \eta_x + [u_1(y=\eta)]_x = 0$, we arrive at the following set of evolution equations governing the weakly nonlinear dynamics:

$$\eta_t + \hat{\alpha}_1\eta_x - \hat{\beta}_1 M\Gamma_{xx} + \hat{\gamma}_1\eta\eta_x - \hat{\chi}_1 M(\eta\Gamma_x)_x = 0, \tag{32}$$

$$\Gamma_t + \hat{\alpha}_2\eta_x - \hat{\beta}_2 M\Gamma_{xx} + \hat{\gamma}_2\eta\eta_x - \hat{\chi}_2 M(\eta\Gamma_x)_x = 0, \tag{33}$$

where the coefficients of the nonlinear parts are given by

$$\hat{\gamma}_1 = \frac{2}{\Delta}(d^3 - d)(1-m), \quad \hat{\chi}_1 = \frac{d}{(m+d)}\left(\frac{(d+1)}{2}\beta + 1\right),$$

$$\hat{\gamma}_2 = \frac{2}{m+d}\left(1 - \frac{6}{\Delta}(m+d)(d^2+d)\right)(1-m), \; \hat{\chi}_2 = \frac{d}{(m+d)}.$$

Equations (32) and (33) only retain quadratic terms for capturing the weakly nonlinear effects; they are only valid when η and Γ are small compared to the layer thickness and the basic surfactant concentration, respectively. Here we do not attempt to exploit detailed features thereof which might require intensive numerical simulations. Rather, we discuss their qualitative aspects, which might provide some insight into behaviour in the weakly nonlinear regime.

As shown in (32) and (33), there are two types of nonlinear terms: $\eta\eta_x$ and $(\eta\Gamma_x)_x$. Effects of $\eta\eta_x$ are twofold. In (32), $\eta\eta_x$ either amplifies or suppresses the interfacial deflections along the interface, depending on the sign of η_x. Also, since $\eta\eta_x$ has

no effect on the interface midpoints ($\eta = 0$) and the maximum/minimum $\eta_x = 0$, the resulting interface wave becomes steepened, making the wavelength become shorter. If the interfacial tension is sufficiently strong, this wave steepening can make the stabilization robust so that instability can be arrested within the weakly nonlinear regime. This is essentially the Kuramoto–Sivashinsky saturation of instability that is commonly found in a variety of contexts in weakly nonlinear dynamics (Kuramoto & Tsuski 1976; Michelson & Sivashinsky 1977; Bachin *et al.* 1983; Frenkel *et al.* 1987). On the other hand, since Γ has already been excited by the shear-flow advection (via $\hat{\alpha}_2\eta_x$ in (33)) in the early stages of the evolution, $\eta\eta_x$ in (33) can exaggerate or lessen the surfactant concentration perturbation, affecting the subsequent interface growth caused by Marangoni forces. Note that the strength of the effects of $\eta\eta_x$ depends on the viscosity difference $(1 - m)$ in view of $\hat{\gamma}_1$ and $\hat{\gamma}_2$. That is, if the viscosities of the two fluids are equal or nearly matched, the $\eta\eta_x$ effects will be absent or become weak. In this case, the weakly nonlinear dynamics will be modulated solely by the Marangoni term $(\eta\Gamma_x)_x$.

The Marangoni term $(\eta\Gamma_x)_x$, noting that both $\hat{\chi}_1$ and $\hat{\chi}_2$ are positive, can again influence the evolution of η and Γ. Since $(\eta\Gamma_x)_x$ comprises both η and Γ_x, the effects can be determined by their phase difference. When Γ_x is in phase with η (or Γ leads η by $\pi/2$), $\eta\Gamma_x \geqslant 0$ throughout the interface, but it has maxima at the interface crests/troughs ($\eta_x = 0$) and minima at the midpoints ($\eta = 0$). As a result, $(\eta\Gamma_x)_x$ increases (decreases) η for $\eta_x > 0$ (< 0). Since it has no influence on the interface midpoints, the effect steepens the interfacial wave, similarly to the way that the Kuramoto–Sivashinsky term $\eta\eta_x$ does. Meanwhile, since Γ leads η by $\pi/2$, $(\eta\Gamma_x)_x$ also promotes (suppresses) the amplitude of Γ for $\Gamma_x < 0\,(>0)$ while it has no influence on $\Gamma = \Gamma_x = 0$. This, in turn, steepens the Γ profile for $\Gamma_x < 0$. Similarly, if Γ_x is out phase with η (or Γ lags behind η by $\pi/2$), the actions of the Marangoni steepening are just the reverse.

BP studied two-layer Couette–Poiseuille flow with surfactant and demonstrated a possible nonlinear saturation of instability. Their analysis includes interfacial tensions so that the Kuramoto–Sivashinsky mechanism could be responsible for the nonlinear saturation. A saturated interfacial wave can be further steepened by the Marangoni flow that might cause the wave to overturn and break, as BP conjectured. This Marangoni steepening can be now understood by the $(\eta\Gamma_x)_x$ effects mentioned above.

As discussed above, both $\eta\eta_x$ and $(\eta\Gamma_x)_x$ have an impact on the development of the interface and surfactant concentration in the weakly nonlinear regime. They mediate the prevailing effects from the linear parts of the evolution equations, or vice versa. On the one hand, $\eta\eta_x$ steepens an interfacial wave; it encourages the surfactant concentration perturbation, and hence the Marangoni effects. But the induced Marangoni effects can also stimulate or reduce the interface growth, depending on which tendency prevails. On the other hand, $(\eta\Gamma_x)_x$ can steepen both η and Γ waves; similar Marangoni modulations again determine the subsequent development of the system. The ultimate fate of the system seems to hinge on the interplay of these effects in the course of the evolution.

Special attention should be paid to the $m = 1$ case in which the $\eta\eta_x$ terms are absent. Inspecting (32) and (33) in line with the linear theory in § 3.2 reveals that the Marangoni terms only participate to stimulate the interface growth, but are of a higher order in (33) that is dictated by the shear-flow term $\hat{\alpha}_2\eta_x$. Thus, $(\eta\Gamma_x)_x$ only steepens the η wave, but not for the Γ profile. The steepened interfacial wave then magnifies the Γ perturbation via the shear-flow term, exaggerating the Marangoni-induced interface growth and exacerbating the instability. We therefore speculate that

such an instability cannot be inhibited by the nonlinear effects; it might still prevail and persist in the nonlinear regime.

5. Concluding remarks

We have provided a rationale for the flow-induced Marangoni instability due to the presence of surfactant. The mechanisms are illuminated by examining the long-wavelength instabilities of both falling film and two-fluid Couette flows. For each flow system, a coupled set of evolution equations for the perturbed interface and surfactant concentration is derived. Both systems produce very similar sets of evolution equations. These equations appear to be in very simple forms that only contain contributions from base flows and Marangoni effects. This not only furnishes a lucid way to clarify the instability mechanisms on an equation basis, but also provides an alternative view of the underlying physics.

A base flow can rearrange the surfactant distribution and induce Marangoni flows to trigger the interface growth, but this destabilizing effect can be reduced by two effects; it is not only offset by the interface travelling motions, but also mitigated by the Marangoni recoil on the surfactant concentration. The competition between these effects determines the occurrence of instability although the presence of base flows is necessary to the Marangoni instability (FH, BP). The interaction among these effects is also identified by examining the initial value problems. More importantly, an instability criterion can be established in line with the same rationale based on these competing effects. A vertically falling film flow is neutrally stable due to surfactant (WJ), but it could be destabilized by imposing shear (Wei 2005*a*). A two-fluid Couette flow with surfactant can be stable or unstable (FH, BP). All these occurrences can be explained using the same framework.

We have demonstrated that the long-wave evolution equations have the advantage of facilitating interpretation. The insight gained from this work can complement the previous studies (WJ, FH, BP). FH and Wei (2005*a*) studied the long-wave stability problem using the standard stream function formulation that could make the interpretation less straightforward. Basically, their proposed instability mechanism was based on the phase difference between the interface and surfactant concentration from the viewpoint of eigenfunctions. BP derived a set of long-wave evolution equations. Although they did not present their equations in a form that would illuminate mechanisms, they numerically identified such a phase difference that is necessary for instability. The present work generalizes these studies; it shows the origin of the phase difference as well as how it triggers the Marangoni interface growth on an equation basis. Moreover, in contrast to these previous studies, we utilize the concept of vorticity to explain instability mechanisms and demonstrate that stability/instability can be explained using the phase difference between vorticity and the interface rather than that between the surfactant concentration and the interface. The explanations given by these previous studies were only for the Marangoni-induced interface growth; reducing effects were not addressed.

In the weakly nonlinear regime, we derived a set of evolution equations relevant to two-layer Couette flow and briefly discuss their qualitative features. Two types of nonlinearity are identified here: the Kuramoto–Sivashinsky and the Marangoni nonlinear terms. Both types of nonlinearity can cause the developments of the interface and surfactant concentration perturbations. In particular, we find that the Marangoni nonlinearity can also steepen waves, similar to the Kuramoto–Sivashinsky term. Since the wave steepening can enhance the Marangoni effects that can either stimulate

or reduce the linear growth, the ultimate fate of the system seems to hinge on the modulation between linear and nonlinear effects.

While the current analysis neglects effects of inertia and surface tension for assessing the interactions between base flows and Marangoni effects, there is no conceptual difficulty in including these effects. However, there is an important aspect that cannot be foreseen by the long-wave analysis. The long-wave analysis predicts that the growth rates increase monotonically with the Marangoni number; it excludes the possibility of a decrease in the growth rate due to the surface immobilization arising from large Marangoni numbers or short wavelengths. This issue might be resolved by either rescaling parameters in the problem, or by extending to the case with arbitrary-wavelength disturbances. For the latter case, since most of the terms appearing in the governing equations and boundary conditions are not simplified, it generally becomes more difficult to identify interactions or dominant effects among various factors even in the limit of Stokes flow (Halpern & Frenkel 2003; Pozrikidis 2003). Nevertheless, as long as the wavelengths of disturbances are not long, inclusion of surface tension effects is almost warranted. For planar systems, surface tension is stabilizing and clearly compromises the Marangoni destabilization. For cylindrical flow systems such as core–annular flows (Wei & Rumschitzki 2005; Wei 2005*b*), however, the flow-induced Marangoni effect could enhance the capillary instability. Applying the evolution-equation approach to these systems could be helpful to reveal the features of their stability.

The research work was supported by the National Science Council of Taiwan under Grant NSC93-2214-E006-021.

REFERENCES

Bachin, A. J., Frenkel, A. L., Levich, B. G. & Sivashinsky, G. I. 1983 Non-linear saturation of Rayleigh-Taylor instability in thin films. *Phys. Fluids* **26**, 3159–3161.

Berg, J. C. & Acrivos, A. 1965 The effect of surface active agents on convection cells induced by surface tension. *Chem. Engng Sci.* **20**, 737–745.

Blyth, M. G. & Pozrikidis, C. 2004 Effect of surfactants on the stability of two-layer channel flow. *J. Fluid Mech.* **505**, 59–86 (referred to herein as BP).

Charru, F. & Hinch, E. J. 2000 'Phase diagram' of interfacial instabilities in a two-layer Couette flow and mechanism of the longwave instability. *J. Fluid Mech.* **414**, 195–223.

Frenkel, A. L., Bachin, A. J., Levich, B. G., Shlang, T. & Sivashinsky, G. I. 1987 Annular flows can keep unstable films from breakup: nonlinear saturation of capillary instability. *J. Colloid Interface Sci.* **115**, 225–233.

Frenkel, A. L. & Halpern, D. 2002 Stokes-flow instability due to interfacial surfactant. *Phys. Fluids* **14**, L45–L48 (referred to herein as FH).

Halpern, D. & Frenkel, A. L. 2003 Destabilization of a creeping flow by interfacial surfactant: Linear theory extended to all wavenumbers. *J. Fluid Mech.* **485**, 191–220.

Hinch, E. J. 1984 A note on the mechanism of the instability at the interface between two shearing flows. *J. Fluid Mech.* **144**, 463–465.

Huang, C. T. & Khomami, B. 2001 The instability mechanism of single and multilayer Newtonian and viscoelastic flows down an inclined plane. *Rheol. Acta* **40**, 467–484.

Kelly, R. E., Goussis, D. A., Lin, S. P. & Hsu, F. K. 1989 The mechanism for surface wave instability in film flow down an inclined plane. *Phys. Fluids* A **1**, 819–828.

Kuramoto, Y. & Tsuzuki, T. 1976 Persistent propagation of concentration waves in dissipative media far from thermal equilibrium. *Prog. Theor. Phys.* **55**, 356–369.

Michelson, D. M. & Sivashinsky, G. I. 1977 Non-linear analysis of hydrodynamic stability in laminar flames. 2. numerical experiments. *Acta Astron.* **4**, 1207–1221.

Pearson, J. R. A. 1958 On convection cells induced by surface tension. *J. Fluid Mech.* **4**, 489–500.

Pozrikidis, C. 2003 Effect of surfactants on film flow down a periodic wall. *J. Fluid Mech.* **496**, 105–127.

Wei, H.-H. 2005*a* Effect of surfactant on the longwave instability of a shear-imposed liquid flow down an inclined plane. *Phys. Fluids* **17**, 012103.

Wei, H.-H. 2005*b* Marangoni destabilization on a core-annular film flow due to the presence of surfactant. *Phys. Fluids* **17**, 027101.

Wei, H.-H. & Rumschitzki, D. S. 2005 Effects of surfactants on the linear stability of core annular flow. *J. Fluid Mech.* (in press).

Whitaker, S. & Jones, L. O. 1966 Stability of falling liquid films. Effect of interface and interfacial mass transport. *AIChE J.* **12**, 421–431 (referred to herein as WJ).

Yih, C. S. 1963 Stability of liquid flow down an inclined plane. *Phys. Fluids* **6**, 321–334.